

X-ray Emission from Haloes of Simulated Disc Galaxies

S. Toft,^{1*} J. Rasmussen¹, J. Sommer-Larsen² and K. Pedersen,¹

¹*Astronomical Observatory, Copenhagen University, Juliane Maries Vej 30, DK-2100 Copenhagen Ø, Denmark*

²*Theoretical Astrophysics Center, Juliane Mariesvej 30, DK-2100 Copenhagen Ø, Denmark*

ABSTRACT

Bolometric and 0.2–2 keV X-ray luminosities of the hot gas haloes of simulated disc galaxies have been calculated at redshift $z=0$. The TreeSPH simulations are fully cosmological and the sample of 44 disc galaxies span a range in characteristic circular speeds of $V_c = 130\text{--}325\text{ km s}^{-1}$. The galaxies have been obtained in simulations with a considerable range of physical parameters, varying the baryonic fraction, the gas metallicity, the meta-galactic UV field, the cosmology, the dark matter type, and also the numerical resolution. The models are found to be in agreement with the (few) relevant X-ray observations available at present. The amount of hot gas in the haloes is also consistent with constraints from pulsar dispersion measures in the Milky Way. Forthcoming XMM and Chandra observations should enable much more stringent tests and provide constraints on the physical parameters. We find that simple cooling flow models over-predict X-ray luminosities by up to two orders of magnitude for high (but still realistic) cooling efficiencies relative to the models presented here. Our results display a clear trend that *increasing* cooling efficiency leads to *decreasing* X-ray luminosities at $z=0$. The reason is found to be that increased cooling efficiency leads to a decreased fraction of hot gas relative to total baryonic mass inside of the virial radius at present. At gas metal abundances of a third solar this hot gas fraction becomes as low as just a few percent. We also find that most of the X-ray emission comes from the inner parts ($r \lesssim 20\text{ kpc}$) of the hot galactic haloes. Finally, we find for realistic choices of the physical parameters that disc galaxy haloes possibly were *more than one order of magnitude* brighter in soft X-ray emission at $z\sim 1$, than at present.

Key words: methods: N-body simulations –cooling flows –galaxies: evolution –galaxies: formation –galaxies: halos –galaxies: spiral –X-rays: galaxies

1 INTRODUCTION

In disc galaxy formation models infall of halo gas onto the disc due to cooling is a generic feature. However, the gas accretion rate and hot gas cooling history are at best uncertain in all models so far. It is thus not clear to which extent the gas cooling out from the galaxy’s halo is replenishing that which is consumed by star formation in the disc. Such continuous gas infall is essential to explain the extended star formation histories of isolated spiral galaxies like the Milky-Way and the most likely explanation of the “G-dwarf problem” — see, e.g., Rocha-Pinto & Marciel (1996) and Pagel (1997).

At the virial temperatures of disc galaxy haloes the dominant cooling mechanism is thermal bremsstrahlung plus atomic line emission. The emissivity, increasing strongly with halo gas density, is expected to peak fairly close to the disc and decrease outwards, and if the cooling rate is signif-

icant the X-ray flux may be visible well beyond the optical radius of a galaxy.

Recently, Benson et al. (2000) compared ROSAT observations of three massive, nearby and highly inclined disc galaxies with predictions of simple cooling flow models of galaxy formation and evolution. They showed that these models predict about *an order of magnitude* more X-ray emission from the galaxy haloes (specifically from a 5–18 arcmin annulus around the galaxies) than observational detections and upper limits.

In this paper we present global X-ray properties of the haloes of a large, novel sample of model disc galaxies at redshift $z=0$. The galaxies result from physically realistic gravity/hydro simulations of disc galaxy formation and evolution in a cosmological context. We find that our model predictions of X-ray properties of disc galaxy haloes are consistent with observational detections and upper limits. Given the results of the theoretical models of Benson et al. we list the most important reasons why simple cooling flow models

* E-mail: toft@astro.ku.dk

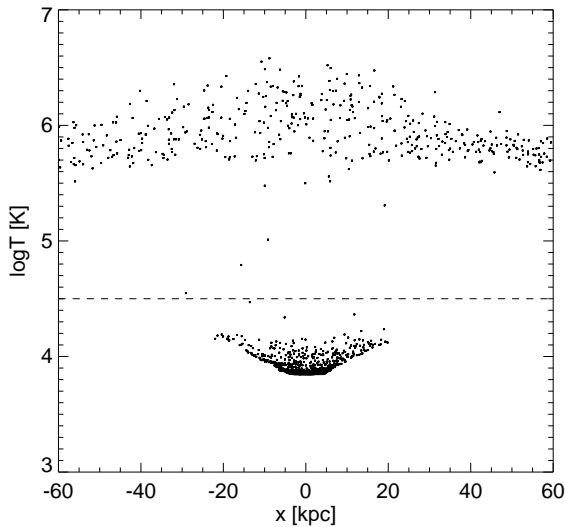


Figure 1. The figure shows the temperature of the SPH gas particles in a typical disc galaxy from our simulations versus their x coordinate (one of the axes in the disc). The “cold” ($\log T < 4.5$) gas which is primarily situated in the disc is removed from the catalogues since it does not contribute to the X-ray flux.

over-predict the present day X-ray emission of disc galaxy haloes.

In section 2 we give a very short description of the disc galaxy simulations. In section 3 we briefly describe the X-ray halo emission calculations and in section 4 the results obtained. Section 5 constitutes the discussion and section 6 the conclusion.

2 DISC GALAXY SIMULATIONS

We have in recent years developed novel models of formation and evolution of disc galaxies. The model disc galaxies result from *ab initio*, fully cosmological ($\Omega_M = 1$ or $\Omega_M + \Omega_\Lambda = 1$), gravity/hydro simulations. These simulations are started at a sufficiently high redshift ($z_i=20-40$) that the density perturbations are still linear and are then evolved through the entire non-linear galaxy formation regime to the present epoch ($z=0$). The code uses a gridless, fully Lagrangian, 3-D TreeSPH code incorporating the effects of radiative cooling and heating (including the effects of a meta-galactic UV field), inverse Compton cooling, star formation, and energetic stellar feedback processes.

A major obstacle in forming realistically sized disc galaxies in such simulations is the so-called “angular momentum problem” (e.g., Navarro & White 1994, Sommer-Larsen et al. 1999). We overcome this problem in two different ways: a) Using cold dark matter (CDM) + stellar feedback processes (Sommer-Larsen et al. 2002) or b) Using warm dark matter (WDM) (Sommer-Larsen & Dolgov 2001). A total of 44 such disc galaxy models with characteristic circular velocities in the range $V_c = 130-325 \text{ km s}^{-1}$ form the basis of the predictions presented in this paper. The simulations initially consist of 30000-400000 SPH+DM particles and in the majority of them some of the SPH particles are turned into star particles over the course of the

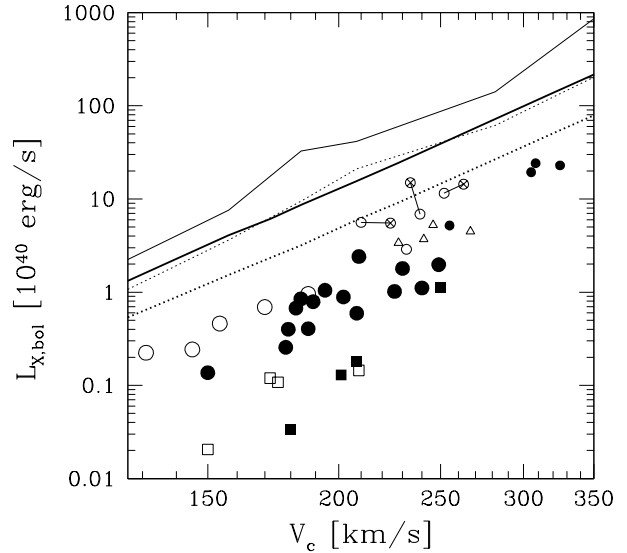


Figure 2. Bolometric luminosity as a function of characteristic circular speed. **Small symbols:** Flat $\Omega_M = 1.0$ cosmology: Open symbols: baryon fraction $f_b=0.05$, filled circles $f_b=0.1$. Triangles: without UV field, non-triangles: with a UV field of the Efstathiou (1992) type. Connected symbols are the same galaxies run with medium (open circles) and high (open circles with crosses) resolution. All simulations represented by small symbols have primordial abundance. **Large symbols:** Flat (Ω_Λ, Ω_M) = (0.7, 0.3) cosmology: Open symbols: $f_b=0.05$, filled symbols $f_b=0.1$. Circles correspond to primordial abundance and with a Haardt & Madau (1996) UV field, squares correspond to $Z = 1/3 Z_\odot$ (using the cooling function of Sutherland & Dopita 1993, which does not include effects of a UV field). The curves are the $L_{X,bol}-V_c$ relationship for the simple cooling flow models (for Λ CDM NFW haloes) described in Sec. 5. The curves represent different baryonic fractions (solid curves have $f_b = 0.1$, dotted curves have $f_b = 0.05$) and abundances (thick curves: primordial abundances, thin curves: $Z = 1/3 Z_\odot$).

simulation — for details about the TreeSPH simulations we refer the reader to the above quoted references.

Most of the simulations were run with primordial gas composition (76% H and 24% He by mass) under the assumption that the inflowing, hot gas is fairly unenriched in heavy elements. To test the effects of metal abundance eight Λ CDM simulations (four with “universal” baryonic fraction $f_b=0.05$ and four with $f_b=0.10$) were run with a gas abundance of 1/3 solar (specifically $[\text{Fe}/\text{H}]=-0.5$). This is the metal abundance of the intracluster medium and can probably be considered a reasonable upper limit to the metal abundance of the hot gas in disc galaxy haloes.

3 X-RAY HALO EMISSION CALCULATION

For each of the simulated galaxies at $z=0$ we create a catalogue of SPH gas particle positions, densities, temperatures and masses. For each catalogue a box of size $(1000 \text{ kpc})^3$ centered on the galaxy is retained and all gas particles with temperatures $\log(T) < 4.5$ are cut away (see Fig. 1) since

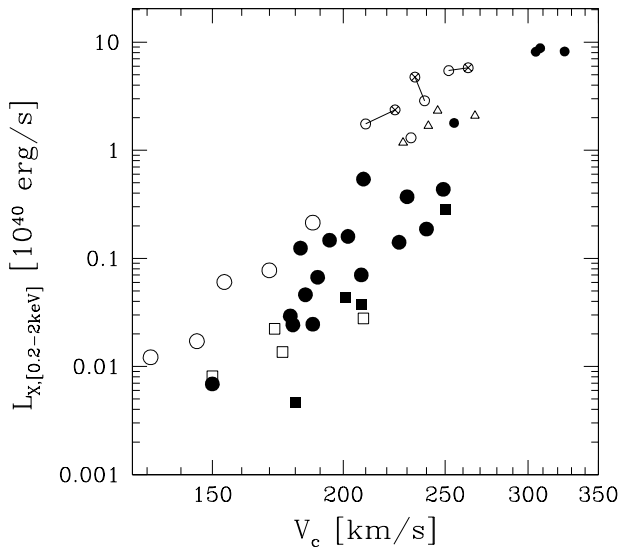


Figure 3. 0.2-2 keV band luminosity as a function of characteristic circular speed. Symbols as in Fig. 2.

they will not contribute to the X-ray flux (these are mainly gas particles which have cooled onto the disc). The density and temperature of each particle is then averaged over itself and its five nearest neighbors using a spherical smoothing kernel proposed by Monaghan & Lattanzio (1985)¹, and a volume is assigned to the particle given its mass and density. Using the average temperatures and densities, each SPH particle is treated as an optically thin thermal plasma, and the associated X-ray luminosity is calculated at the relevant position in a given photon energy band with the *meke* plasma emissivity code (Mewe et al. 1986). X-ray luminosities are then computed by summation over all particles in the volume of interest. The bolometric X-ray luminosity is calculated using the 0.012 – 12.4 keV band.

4 RESULTS

In Fig. 2 the total bolometric X-ray luminosities $L_{X,bol}$ of the 44 simulated disc galaxies in our sample are plotted versus their characteristic circular speed V_c , defined as the circular velocity in the disc at $R_{2.2} = 2.2 R_d$, where R_d is the disc scale length – see Sommer-Larsen & Dolgov (2001) for details. The X-ray luminosities derived from the simulations are up to two orders of magnitude below values derived from simple cooling flow models which are described in Sec. 5.1. As can be seen from the figure $L_{X,bol} \sim 10^{40} \text{ erg s}^{-1}$ for a Milky Way sized galaxy.

As expected from the simple models, the simulated

¹ It is important to note that we average over the *original* densities from the TreeSPH simulations. One can show that if the cold gas particles are cut away and the densities of the remaining gas particles are then recalculated using the full SPH procedure the X-ray luminosities will be underestimated due to resolution problems at the disc-halo interface.

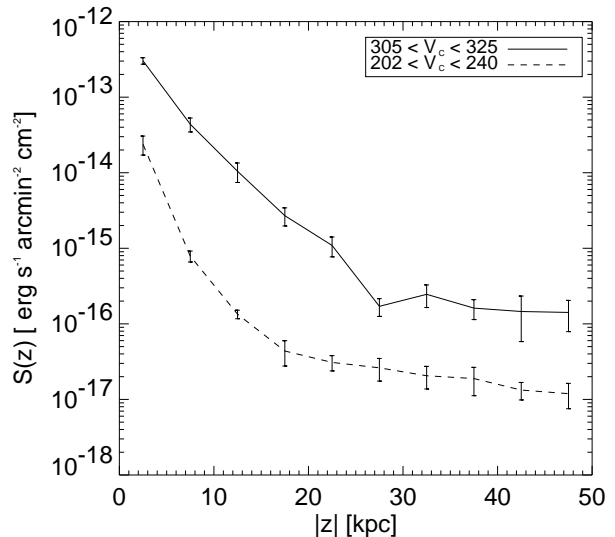


Figure 4. Mean bolometric X-ray surface brightness profiles perpendicular to the plane of the disc of three high V_c galaxies (solid curve) and four Milky Way sized galaxies (dashed curve). The physically most important parameters for these galaxies are $f_b=0.10$ and primordial gas abundance. The profiles were calculated by binning the emission in 40 kpc wide, 5 kpc high slices parallel to the disc.

galaxies display an $L_{X,bol}-V_c$ relation, but with a significant scatter. Part of this scatter arises from the different conditions under which the simulations have been run (see Sec. 5.3) and part of it is a “real” scatter arising from the different geometries and cooling histories of the individual galaxy haloes. This “real” scatter can be estimated by inspection of the large filled circles in Fig. 2 which represent simulations run with the same, physically important parameters (see the figure caption). These data points display a rms dispersion of about 50% around the mean.

There is a tendency for galaxies formed in simulations with baryon fraction $f_b=0.05$ and primordial gas abundance to have systematically higher $L_{X,bol}$ (by about a factor of two) than galaxies formed in similar simulations with $f_b=0.10$. Also, galaxies formed in simulations with gas abundance $Z = 1/3 Z_\odot$ tend to have systematically lower $L_{X,bol}$ than the ones with primordial gas. We discuss these trends in Sec. 5.

Fig. 3 shows the 0.2-2 keV band X-ray luminosities of the 44 sample disc galaxies versus V_c . The systematic trends mentioned above are also seen in this plot, in particular is the difference between the $f_b=0.05$ and 0.10 simulations (with primordial gas) even more pronounced than in Fig. 2. We also discuss this in Sec. 5.

Most (but not all) of the X-ray emission originates from regions of the hot gas halo fairly close to the disc: 95% of the emission typically originates within about 20 kpc of the disc. This is illustrated in Fig. 4 where we plot the mean surface brightness profiles perpendicular to the disc of three high V_c galaxies and four Milky Way sized galaxies.

5 DISCUSSION

5.1 Comparison to simple cooling flow models

In order to compare our results with previous work, we calculated a family of simple cooling flow models similar to those considered by Benson et al. (2000).

In these models it is assumed that the cooling occurs in a static potential and that the gas initially was in place and traced the dark matter (DM). Gas is assumed to flow from the cooling radius (at which the cooling time equals the age of the universe) to the disc (settling there as cold gas) on a time-scale much shorter than the Hubble time. The bolometric X-ray luminosity can then be approximated simply as the mass accretion rate, $\dot{M}_{\text{cool}} = 4\pi r_{\text{cool}}^2 \rho_{\text{gas}}(r_{\text{cool}}) \dot{r}_{\text{cool}}$, times the gravitational potential difference, so

$$L_{X,\text{bol}} = \dot{M}_{\text{cool}}(r_{\text{cool}}) \int_{r_{\text{optical}}}^{r_{\text{cool}}} \frac{V_c^2(r)}{r} dr. \quad (1)$$

In Fig. 2 we show for different baryonic fractions and halo gas metallicities the $L_{X,\text{bol}}-V_c$ relationships expected from such simple models for haloes of the Λ CDM NFW types (Navarro, Frenk & White 1996) - the relationships for SCDM NFW haloes are very similar. Effects of a meta-galactic UV field were not included in these simple models — such effects are less significant than the effects of varying the baryon fraction and the gas abundance.

The disc galaxies resulting from our simulations follow an $L_{X,\text{bol}}-V_c$ relation with approximately the same slope as the relation derived from simple cooling flow models ($L_{X,\text{bol}} \propto V_c^5$ - see Fig. 2), but shifted to systematically lower $L_{X,\text{bol}}$ and with a significant scatter. At small V_c the relation looks steeper, but this can be attributed to the systematically lower $L_{X,\text{bol}}$ of galaxies formed in simulations with a uniform gas abundance of 1/3 solar rather than primordial - see sec. 5.3.3.

The main reasons why the simple cooling flow models predict up to two orders of magnitude more X-ray luminosity than the physically more realistic simulated galaxies considered here are:

(i) The assumption that the DM potential is static and that all gas is in place at the beginning of the galaxy's history, tracing the assumed static DM halo. In our simulations the distribution of gas in the DM haloes is dynamic in the sense that it changes due to discrete merging and interaction events, especially in the early phases of the simulations, $z \gtrsim 1-2$.

(ii) The assumption that gas particles at the cooling radius instantly cool out from a static infinite reservoir of hot gas. The gas halo profile is continuously changing everywhere in the halo as the hot gas cools out, not just at the cooling radius. Moreover, only the hot gas inside of the virial radius is available for disc formation — the effect of this in cases of high cooling efficiency is very significant as discussed in section 5.3.

(iii) The bulk of the cooling and X-ray emission is determined by what is going on fairly close to the disc ($r \lesssim 20\text{kpc}$) rather than what is happening at the cooling radius (see Fig.4).

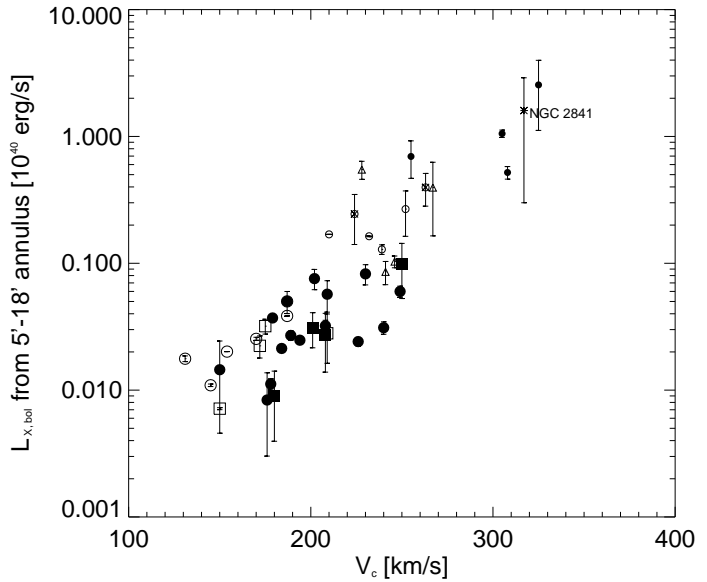


Figure 5. Bolometric luminosity in the annulus considered by Benson et al. (2000) (a ring around the galaxy, with an inner radius of 5 arcmin and an outer radius of 18 arcmin) of all the disc galaxies in our simulation sample (assuming a distance of 13.8 Mpc). All galaxies are viewed “edge on”, the error bars represents the difference in L_X resulting from viewing the galaxies along the x and y directions, respectively. The observed data point (indicated by an asterisk) and its error bars are adopted from Benson et al. Other symbols as in Fig. 2.

5.2 Comparison to observations

When trying to determine the amount of X-ray halo emission observationally, it is important not to confuse the signature of cooling, hot gas with the emission from X-ray binaries in the disc, the diffuse emission of the galaxy's disc (Read, Ponman & Strickland 1997), or with the X-ray emission from hot bubbles of outflowing gas that is seen in starburst galaxies (see Pietch et al. 1997 and Strickland & Stevens 2000).

In a recent deep Chandra observation of a nearby edge-on spiral galaxy NGC 4631 soft X-ray emission extending up to 7 kpc from the disc was observed (Wang et al. 2001). However, this disc is disturbed due to interaction and the off-disc emission was attributed to processes in the disc.

Benson et al. (2000) attempted to detect diffuse halo emission in deep ROSAT observations of the haloes of three large and nearly edge-on, isolated and undisturbed disc galaxies; NGC 2841, NGC 4594 and NGC 5529. This study was limited by the sensitivity, and poor point source removal possible with ROSAT, but despite this the authors were able to place limits on the X-ray emission in an annulus around the galaxies (with an inner radius of 5 arcmin and an outer radius of 18 arcmin). Of the three galaxies considered the strongest constraint was derived for the halo of the relatively nearby (distance 13.8 ± 5.2 Mpc) massive ($V_c = 317 \pm 2 \text{ km s}^{-1}$) disc galaxy NGC 2841. In the annulus around this galaxy a bolometric luminosity of $L_X = 1.6 \pm 1.3 \times 10^{40} \text{ erg s}^{-1}$ was derived. This is much less than expected from the simple cooling-flow models. Benson et al. (2000) predict (assuming $f_b=0.06$ and $Z=0.3 Z_\odot$) the luminosity in this annulus to be about 30 times higher;

$L_X = 45 \pm 4.4 \times 10^{40} \text{ erg s}^{-1}$ for NFW haloes (and even more for isothermal sphere haloes). However, the above result is in excellent agreement with the expectation from our simulations, as illustrated in Fig. 5 where we plot the bolometric luminosity in the considered annulus (assuming a distance of 13.8 Mpc) of all the galaxies in our simulation sample versus V_c . We note that our three “data” points at $V_c=300\text{--}325 \text{ km s}^{-1}$ are for simulations with baryon fraction $f_b=0.10$ and primordial gas abundance. For a *given* V_c we would expect the bolometric luminosities to be about twice as much for simulations with $f_b=0.05$ - see section 5.3.4. Such a low f_b is unlikely given determinations of the “universal” baryon fraction, $f_b \approx 0.10 (h/0.7)^{-3/2}$, derived from galaxy clusters (Ettori & Fabian 1999) and galaxy clustering (Percival et al. 2001), but in any case the X-ray luminosities would still be consistent with the NGC 2841 measurement. Moreover, the (more realistic) inclusion of some level of enrichment in the gas and the use of the more realistic meta-galactic UV field of Haardt & Madau (1996) would tend to *lower* the X-ray luminosities. We also note that the total X-ray luminosities of our three galaxies at $V_c=300\text{--}325 \text{ km s}^{-1}$ are “only” a factor of 3–5 lower than the predictions of the simple cooling flow models of Benson et al. and ours (the latter for $f_b=0.10$ and primordial gas). Hence an important part of the reason why our models match the observed bolometric luminosity of the 5–18 arcmin annulus around NGC 2841 is that most of the X-rays are emitted from the inner 20 kpc of our model disc galaxy haloes (5 arcmin correspond to 20 kpc at a distance of 13.8 Mpc). In other words our “geometric correction” is considerably larger than the one used by Benson et al.

The observational constraints on the bolometric luminosity of NGC 4594 and NGC 5529 are weaker than for NGC 2841. The upper limits on these are again about an order of magnitude less than expected from the simple models, but in agreement with the expectation from our simulations.

The diffuse X-ray luminosity of the Milky Way’s hot halo has recently been estimated: Pietz et al. (1998) estimate a 0.1–2 keV luminosity of $7 \cdot 10^{39} \text{ erg s}^{-1}$ and Wang (1997) a 0.5–2 keV luminosity of $3 \cdot 10^{39} \text{ erg s}^{-1}$. Assuming a temperature of 0.15 keV (Georgantopoulos et al. 1996; Parmar et al. 1999) this translates into 0.2–2 keV luminosities of 5 and $7 \cdot 10^{39} \text{ erg s}^{-1}$ respectively. These estimates (which should probably be seen as upper limits) are consistent with our findings from the simulations for $V_c \simeq 220 \text{ km s}^{-1}$ — see Fig. 3.

5.3 Effects of numerical resolution and physical parameters

The galaxies in our sample have been compiled from a number of simulations which have been run with different cosmological and environmental parameters. These inhomogeneities in our simulation sample may introduce some scatter in the $L_X - V_c$ diagram. On the other hand, this allows us to investigate trends when varying the physical parameters.

In general, varying a parameter has impact on the present day X-ray luminosity of a given galaxy if it significantly alters the ability of the hot halo gas to cool during its life time. In the simple cooling flow models, increasing the cooling efficiency leads to an increase in L_X , while this is not necessarily the case in more realistic simulations. If

the cooling efficiency is increased, more gas has cooled out on the disc at $z = 0$. This results in an increase of the characteristic circular speed of the disc as its dynamics become more baryon (and less DM) dominated, and usually a *decrease* in the X-ray luminosity of the halo since there is less hot gas left in the halo to cool and contribute to the X-ray emission.

In the following we briefly discuss how the derived results depend on the resolution of the simulation, the presence of an external UV field, the assumed gas metallicity, the baryon fraction f_b , the cosmology, the dark matter type and whether or not star formation is incorporated in the simulations.

5.3.1 Effects of resolution

An important test of all numerical simulations is to check whether the results depend on the resolution. This can be done from Fig. 2 by comparing the connected symbols. These represent the same galaxy, run with normal (open symbols) and 8 times higher mass + 2 times higher force resolution (open symbols with crosses). It can be seen that this significant increase in resolution only leads to a very modest increase of $19 \pm 64 \%$ in the X-ray luminosity relative to the mean $L_X - V_c$ relation (i.e. taking the effect of the change of V_c with resolution into account). A similar result is inferred from Fig. 3.

5.3.2 Effects of a meta-galactic UV field

The main effects of a hard UV photon field is to ionize the gas, significantly reducing its ability to cool by collisional excitation (line-cooling) mechanisms (Vedel, Hellsten and Sommer-Larsen 1994). This effect is evident in Fig. 2 where the set of 4 small triangles and the set of 4 small open circles represent the same 4 haloes, run under exactly the same conditions, except that for the latter effects of a meta-galactic, redshift-dependent UV field were included in the cooling/heating function. There is a tendency for the galaxies without an external UV-field to have lower $L_{X,bol}$ and higher V_c than the galaxies with external UV-field: The former have a median bolometric luminosity of $55 \pm 16\%$ of the latter (again taking into account the change of V_c).

So in this case an increase in the cooling rate leads to a decrease in $L_{X,bol}$ at the present epoch since a smaller amount of hot gas is left in the halo to produce the emission — see Fig. 6. Note however that in the above simulations with UV field we used a field of the Efstathiou (1992) type which is too hard and intense compared to the more realistic one of Haardt & Madau (1996) — see also Sec. 5.3.5. Hence, the suppression in cooling efficiency and the related increase in $L_{X,bol}$ for disc galaxy haloes formed in simulations with a Efstathiou type UV field is somewhat too large.

5.3.3 Effects of gas metallicity

The effects of the metallicity of the gas on the derived $L_{X,bol}$ can be investigated by comparing the squares in Fig. 2 (which have $Z = 1/3 Z_\odot$) with the rest of the symbols (which have primordial abundance). In the simple cooling flow models, an increase of the metal abundance leads to an increase in

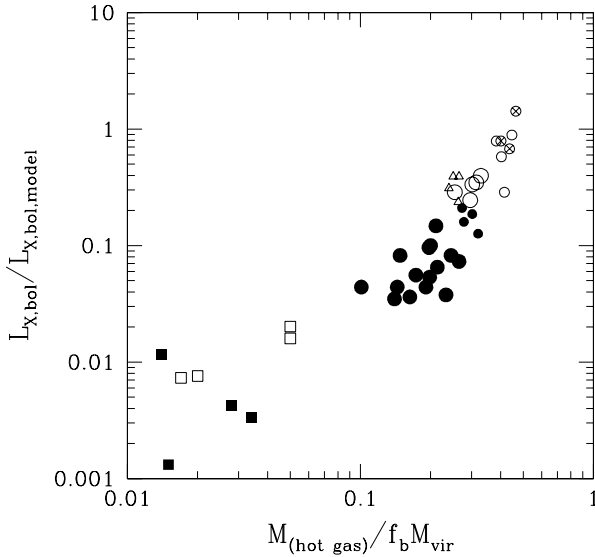


Figure 6. Bolometric luminosity relative to the one expected for the simple cooling flow models versus hot gas fraction - see text for details. Symbols as in Fig. 2.

the cooling rate and $L_{X,bol}$ (compare the thick and thin curves in Fig. 2); however this is not what we find from our simulations. The galaxies with $Z = 1/3 Z_\odot$ have systematically lower $L_{X,bol}$ than the galaxies with primordial abundance, by about a factor of 3-4 for the same f_b . This is in agreement with the argument that increasing the cooling efficiency leads to a decrease in $L_{X,bol}$ at $z = 0$. Note that for the $Z = 1/3 Z_\odot$ simulations we used the cooling function of Sutherland & Dopita (1993) which does not include the effect of a UV field. So we can not completely disentangle the effects of gas metal abundance versus lack of UV field on the X-ray luminosities, but Fig. 6 strongly hints that the former is the most important.

5.3.4 Effects of baryon fraction

Comparing in Fig. 2 $L_{X,bol}$ for simulations run with primordial gas and with $f_b=0.05$ and 0.10 , respectively, the former are more luminous on average by about a factor of two. Yet again we see how increased cooling efficiency leads to a decreased $L_{X,bol}$ at $z=0$.

Summarizing the above results we find no statistically significant dependence of the X-ray luminosities of the simulated galaxies on numerical resolution. With respect to cooling efficiency there is a general trend of higher cooling efficiency over the course of the simulation to result in less hot gas left in the halo at $z=0$ to cool, yielding a lower X-ray luminosity. This is qualitatively demonstrated in Fig. 6, which shows the bolometric luminosity relative to the one expected for the simple cooling flow models versus the hot gas fraction $f_{(hot\ gas)} = M_{(hot\ gas)}(< r_{vir})/(f_b M_{vir})$, where $M_{(hot\ gas)}(< r_{vir})$ is the mass of hot gas ($\log(T) > 4.5$) inside

of the virial radius r_{vir} and M_{vir} is the total mass (baryonic + DM) inside r_{vir} . It is seen that only for hot gas fractions $f_{(hot\ gas)} \gtrsim 0.4-0.5$, requiring a physically implausible parameter combination of $f_b=0.05$, primordial gas and an unrealistically hard and intense UV field, can our models match the $L_{X,bol}$ predicted by the simple cooling flow models.

Pulsar dispersion measures can be used to place observational upper limits on the amount of hot gas in the halo of the Milky Way. We find from our simulations that Milky Way sized galaxies formed in primordial gas simulations have about $10^9 M_\odot$ of hot gas inside of 50 kpc at $z=0$ and the ones from the $Z = 1/3 Z_\odot$ simulations about $10^8 M_\odot$. Both values are consistent with the observational upper limits of about $2 \cdot 10^9 M_\odot$ from pulsar dispersion measures to the Magellanic Clouds and the globular cluster M53 (Moore & Davis 1994; Rasmussen 2000).

The difference between the $f_b=0.05$ and 0.10 cases is even more pronounced for the 0.2-2 keV X-ray luminosities, as shown in Fig. 3. The reason is that at a *given* characteristic circular speed V_c the dynamics of the inner galaxy (where V_c is determined) are more baryon dominated for $f_b=0.10$ than for $f_b=0.05$. This in turn means that the hot halo is smaller and cooler for the $f_b=0.10$ case than for the $f_b=0.05$ case. This is demonstrated in Fig. 7, which shows the average temperature of the central hot halo gas (inside of $20 h^{-1}$ kpc) for the 44 simulations. At a given V_c the temperature of the inner, hot halo is systematically shifted to lower values for $f_b=0.10$ as compared to $f_b=0.05$. Hence for the relevant, relatively low temperatures ($T \lesssim 0.3$ keV, or equivalently, $V_c \lesssim 300$ km s $^{-1}$) less of the emitted radiation has energies above 0.2 keV for the former than for the latter case. On the issue of baryon dominance of the inner galaxy dynamics note that for a *given* DM halo, $f_b=0.10$ (as compared to $f_b=0.05$) leads to a larger V_c and a smaller $dv_c(R)/dR$ in the outer parts of the disc, where $v_c(R)$ is the rotation curve – this is in line with the findings of Persic, Salucci & Stel (1996) on the basis of a large observational sample of disc galaxy rotation curves.

Finally, as mentioned in Sec. 5.2, the temperature of the Milky Way's inner halo is about 0.15 keV corresponding to $1.5-2 \cdot 10^6$ K in agreement with Fig. 7.

5.3.5 Effects of dark matter type, cosmology and star formation

We do not find any dependence on the DM type, i.e. whether the simulations are of the WDM or CDM + feedback type. Neither do we find any indications of systematic trends with cosmology (SCDM/WDM versus Λ CDM/WDM) although more overlap in figures 2 and 3 between the two cosmologies would have been desirable (the reason for this lack of overlap is that rather different cosmological volumes were sampled in the two cosmologies — the box size was $\sim 40 h^{-1}$ Mpc for the $\Omega_M=1$ cosmology and $10 h^{-1}$ Mpc for the Λ -cosmology). Note also that in Fig. 6 the results for the different cosmologies fall along the same continuous sequence. The reason why the disc galaxies formed in primordial gas simulations for the $\Omega_m = 1$ cosmology tend to have slightly higher relative bolometric luminosity *and* $f_{(hot\ gas)}$ than the Λ -cosmology ones is most likely due to the two different models of the

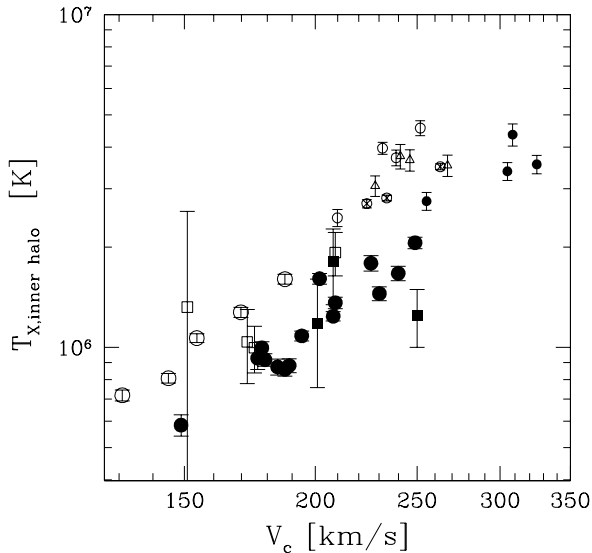


Figure 7. Average inner halo hot gas temperature versus characteristic circular speed - see text for details. Symbols as in Fig. 2.

meta-galactic UV field used: For the former we used the one suggested by Efstathiou (1992) (see Vedel et al. 1994), whereas for the latter we used the more realistic one from Haardt & Madau (1996). The former has $z_{\text{reionization}} = \infty$ and is considerably harder and, at $z \gtrsim 2$, more intense than the latter which has $z_{\text{reionization}} \simeq 6$.

Finally, we do not find any dependence on whether star formation is included or not in the simulations.

5.4 Mass accretion rates

In Sommer-Larsen et al. (2002) disc gas accretion rates due to cooling-out of hot gas are determined for the Λ CDM + feedback model disc galaxies considered there (a subset of the sample considered here obtained in simulations with $f_b=0.10$, primordial gas composition and the Haardt & Madau UV field). For Milky-Way sized galaxies accretion rates in the range $0.3\text{--}0.6 h^{-1} M_{\odot} \text{yr}^{-1}$ ($h=0.65$) are found at $z=0$. One can show that the rate at which hot halo gas cools out is proportional to $L_{X,\text{bol}} < \frac{1}{T} >$, where $< \frac{1}{T} >$ is the emissivity weighted inverse temperature of the hot gas. As mentioned previously we find in the current work that $L_{X,\text{bol}}$ is proportional to about the fifth power of V_c , so as $T \propto V_c^2$ we would expect $\dot{M} \propto V_c^3$. This is indeed found by Sommer-Larsen et al. (2002) and is sensible since the I -band (and hence approximately mass) Tully-Fisher relation has a logarithmic slope of about three (Giovanelli et al. 1997).

Given the trends of L_X with various environmental parameters discussed in section 5.3 we would expect galaxies formed in simulations with $f_b=0.05$ and primordial abundance to have about twice as large mass accretion rates, whereas galaxies formed in $Z = 1/3 Z_{\odot}$ simulations will have accretion rates 3-4 times lower than the similar primordial gas ones. Hence we expect at $z=0$ a fairly strong trend of the ratio of present to average past accretion rate *decreas-*

ing with *increasing* cooling efficiency. Indeed Sommer-Larsen et al. (2002) find for their Λ CDM simulations accretion rates at $z=1$ which are an order of magnitude larger than the ones at $z=0$, so disc galaxies may have been considerably more X-ray luminous in the past than they are today.

A detailed analysis of mass accretion rates and high- z X-ray properties of our sample of simulated disc galaxies will be presented in a forthcoming paper.

5.5 Future X-ray observational tests

From the predicted X-ray surface brightness profiles (Fig.4) and the halo temperatures (Fig.7) we have estimated the feasibility for detecting halo emission with XMM-Newton and Chandra using the most recent instrument responses. In order to avoid confusion with X-ray emission originating in the disc we aim at detecting halo emission from nearly edge-on disc galaxies at (vertical) disc heights of 10-15 kpc. Count rates for a 5 kpc high and 40 kpc wide slice (parallel to the disc) at such disc heights were calculated assuming a column density of absorbing neutral hydrogen in the disc of the Milky Way of $n_H = 2.5 \cdot 10^{20} \text{ cm}^{-2}$ (corresponding to the typical value for galactic latitudes of $|b| \sim 60^\circ$). For galaxies with circular speeds in excess of 300 km s^{-1} and distances $d \lesssim 50 \text{ Mpc}$ XMM-Newton, should be able to obtain a 5σ detection at such disc heights in a 10 ksec exposure. Although Chandra has a smaller collecting area than XMM-Newton the Chandra background is generally lower and its superior spatial resolution allows for more efficient removal of contaminating point sources. We thus expect that only slightly longer exposures are required for Chandra detection of halo emission than for XMM-Newton.

However, the curve in Fig.4 for the $V_c > 300 \text{ km s}^{-1}$ galaxies represents an optimistic case since the underlying simulations were run with primordial abundances and a strong external UV-field, both increasing the present day X-ray luminosity. As mentioned in sections 5.3.2 and 5.3.3, in more realistic simulations, including metals and a weaker external UV-field, the halo flux is lower by a factor of about 3. In this case, XMM-Newton as well as Chandra should still obtain a 5σ detection for $V_c > 300 \text{ km s}^{-1}$ galaxies within 25 Mpc in about 25 ksecs.

For Milky Way sized galaxies, due to their much lower surface brightness (e.g. Fig.4) and lower halo temperature (the latter making these more sensitive to absorption) the predicted XMM-Newton and Chandra halo count rates are two orders of magnitude lower than for the $V_c > 300 \text{ km s}^{-1}$ galaxies. Detection of X-ray haloes for Milky Way sized galaxies at vertical disc heights of 10-15 kpc will thus have to await future X-ray observatories with much larger collecting areas (Constellation-X and XEUS).

6 CONCLUSION

We have presented X-ray properties of the hot gas haloes of disc galaxies derived from a large sample of physically realistic gravity/hydro simulations of galaxy formation and evolution.

The simulated galaxies follow an $L_{X,\text{bol}}\text{--}V_c$ relation with approximately the same slope as expected from simple cooling flow models ($L_{X,\text{bol}} \propto V_c^5$), but shifted to lower $L_{X,\text{bol}}$,

and with a significant scatter (approximately a 50% rms dispersion for a given choice of physical parameters).

The total bolometric X-ray luminosities of the disc galaxy haloes are up to two orders of magnitude less than predicted by simple cooling flow models. Hence, contrary to the order of magnitude discrepancy between simple cooling flow models and observations found by Benson et al. (2000), our models are in agreement with ROSAT observations of the three massive highly inclined spirals NGC 2841, NGC 4594 and NGC 5529. Furthermore, we find that our models are consistent with recent estimates of the diffuse 0.2-2 keV X-ray luminosity of the Milky Way, and also that the amount of hot gas in the haloes of our simulated, Milky Way sized disc galaxies is consistent with upper limits from pulsar dispersion measures toward the Magellanic Clouds and the globular cluster M53.

In contrast to what is predicted by simple cooling flow models, we find that *increasing* the cooling efficiency of the halo gas leads to a *decrease* in the present day L_X . The reason for this is that increasing the cooling efficiency over the course of a simulation results in less hot gas in the halo at $z=0$ to cool (because the total amount of gas available at any given time is always limited to the gas inside of the virial radius). This in turn leads to lower present day accretion rates and lower $L_{X,bol}$. The two most important physical parameters controlling the X-ray luminosities are the baryon fraction and the gas abundance: for a *given* characteristic circular speed V_c , increasing the baryon fraction from $f_b=0.05$ to $f_b=0.1$ decreases $L_{X,bol}$ by a factor of about two, and similarly increasing the gas abundance from primordial to $Z = 1/3 Z_\odot$ results in a decrease in $L_{X,bol}$ of a factor 3-4.

Concerning the spatial distribution of X-ray emission in the hot gas haloes we find that this is centrally concentrated: about 95% of the emission originates within the inner $r \lesssim 20$ kpc.

For their Λ CDM, $f_b=0.1$ and primordial gas abundance simulations Sommer-Larsen et al. (2002) find present day mass accretion rates of $0.5\text{--}1 M_\odot \text{yr}^{-1}$ for Milky Way sized disc galaxies, compatible with observational limits (J. Silk, private communication). As the mass accretion rate effectively is proportional to $L_{X,bol}$ one would expect even lower accretion rates for the more realistic case of some level of metal enrichment of the hot gas. Furthermore, Sommer-Larsen et al. (2002) find mass accretion rates which are an order of magnitude larger at redshift $z \sim 1$. Hence it is quite likely that disc galaxies were considerably X-ray brighter in the past.

Forthcoming XMM-Newton and Chandra observations of massive, nearby, edge-on disc galaxies will provide constraints on the present models, in particular the main physical parameters: the baryon fraction and the hot gas abundance. Future observations to redshifts $z \gtrsim 1$ may be used to constrain the models further.

ACKNOWLEDGMENTS

This project was supported by the Danish Natural Science Research Council (SNF) and by Danmarks Grundforskningsfond through its support for the establishment of the Theoretical Astrophysics Center. We thank R. Bower, M.

Götz, B. Moore, L. Portinari and J. Silk for useful discussions.

REFERENCES

- Benson, A. J., Bower, R. G., Frenk, C.S., White, S. D. M., 2000, MNRAS, 314, 557
- Efstathiou, G., 1992, MNRAS, 256, P43
- Ettori, S., Fabian, A.C., 1999, MNRAS, 305, 834
- Giovannelli, R., et al. 1997, ApJ, 477, L1
- Georgantopoulos, I., Stewart, G.C., Shanks, T., Boyle, B.J., Griffiths, R.E. 1996, MNRAS, 280, 276
- Haardt, F., Madau, P., 1996, ApJ, 461, 20
- Monaghan, J.J., Lattanzio, J.C., 1985, A&A, 149, 135
- Moore, B., Davis, M., 1994, MNRAS, 270, 209
- Mewe, R., Lemen, J.R., van den Oord, G.H.J., 1986, A&A, 65, 511
- Navarro, J. F., White, S. D. M., 1994, MNRAS, 267, 401
- Navarro, J. F., Frenk C. S., White, S. D. M., 1996, ApJ, 462, 563
- Pagel, B. E. J., 1997, Nucleosynthesis and Chemical Evolution of Galaxies (Cambridge: Cambridge Univ. Press)
- Parmar, A.N., Guainazzi, M., Oosterbroek, T., Orr, A., Favata, F., Lumb, D., Malizia, A. 1999, A & A, 345, 611
- Percival, W.J. et al., 2001, MNRAS, 327, 1297
- Persic, M., Salucci, P., Stel, F., 1996, MNRAS, 281, 27
- Pietsch, W. et al., 2001, MNRAS, 365, L174
- Pietz, J. et al., 1998, A&A, 332, 55
- Rasmussen, J., 2000, Master Thesis, University of Copenhagen
- Read, A.M., Ponman, T.J., Strickland, D. K., 1997, MNRAS, 286, 626
- Rocha-Pinto, H. J., Maciel, W. J., 1996, MNRAS, 273, 447
- Sommer-Larsen, J., Dolgov, A., 2001, ApJ, 551, 608
- Sommer-Larsen, J., Gelato, S., Vedel, H., 1999, ApJ, 519, 501
- Sommer-Larsen, J., Götz, M., Portinari, L., 2002, in preparation
- Strickland, D. K., Stevens, I. R., 2000, MNRAS, 314, 511
- Sutherland, R. S., Dopita, M. A., 1993, ApJS, 88, 253
- Vedel, H., Hellsten, U., Sommer-Larsen, J. 1994, MNRAS, 271, 743
- Wang, Q., 1997, astro-ph/9710144
- Wang, Q. et al., 2001, ApJ, 555, L99